Wide- and Small-Angle X-ray Analysis of Poly(ethylene-*co*-octene)

R. Androsch,† J. Blackwell,*,‡ S. N. Chvalun,‡,§ and B. Wunderlich†

Department of Chemistry, The University of Tennessee, Knoxville, Tennessee 37996-1600, and Oak Ridge National Laboratory, Oak Ridge, Tennessee 37831-6197, and Department of Macromolecular Science, Case Western Reserve University, Cleveland, Ohio 44106-4202

Received November 25, 1998; Revised Manuscript Received April 8, 1999

ABSTRACT: Wide-angle X-ray data point to a three-phase structure in isotropic and drawn specimens of a homogeneous poly(ethylene-*co*-octene) (7.3 mol % 1-octene). In addition to the amorphous halo, the unoriented polymer exhibits Bragg reflections characteristic of the orthorhombic crystalline phase and an additional reflection that is assigned to the hexagonal mesophase. On stretching 800%, the degree of crystallinity increases from ∼25% to ∼50%, due mainly to the formation of smaller hexagonal crystallites, while the proportions of the orthorhombic and amorphous phases decline. Small-angle X-ray data reveal a distinct long period, pointing to the existence of lamellae that become oriented perpendicular to the draw direction. On releasing the specimen, there is a considerable permanent set (∼350% extension), and the crystallinity declines to ∼30% as the hexagonal crystallites appear to revert to the amorphous structure. The results suggest that the hexagonal mesophase is formed by chain segments that have octene side chains, once these segments become oriented by deformation.

1. Introduction

A range of linear low-density polyethylenes (LLDPEs) has been produced by metallocene-catalyzed copolymerization of ethylene and various linear 1-alkenes. The densities and other properties of these polymers are determined by the choice of the comonomer ratio and the branch chain length. Typical preparations incorporate up to ∼15 mol % of 1-hexene or 1-octene as random comonomers: they can exhibit low degrees of crystallinity and elastomeric properties. This paper addresses the structure and morphology of one of these materials containing 7.3 mol % 1-octene, with a density of 0.87 g/cm^3. Previous studies of the structure of poly(ethylene-*co*-octene) have pointed to a semicrystalline character, and evidence has been presented for a complex multiphase structure. McFaddin et al.[1] have proposed a three-phase structure based on ^{13}C solid-state nuclear magnetic resonance (NMR) and wide-angle X-ray scattering (WAXS) analyses. An ethylene copolymer with 15 mol % octene gave rise to a WAXS amorphous halo at $2\theta = 20°$ (Cu Kα radiation) containing ∼80% of the total scattered intensity, but they also detected an additional peak or halo at $2\theta = 19.7°$. They assigned the latter scattering to a fraction with order intermediate between crystalline and amorphous, which they suggested contained segments with preferred trans conformations based on NMR data.

Mathot et al.[2,3] have analyzed the structure of homogeneous ethylene−octene copolymers by differential scanning calorimetry (DSC) and X-ray methods. They point to a correlation between the melting point distribution (i.e., the crystallite size distribution) and the ethylene sequence length distribution. They did not detect the orthorhombic form in the WAXS data for a sample with 13.6 mol % octene content (density 0.87 g/cm^3), but both small-angle X-ray scattering (SAXS) and DSC pointed to the existence of an ordered phase, which they suggested consisted of small and imperfect crystallites. However, they also commented on the sharpness of the amorphous halo in the WAXS data, as reported by McFaddin et al.[1]

Minick et al.[4] and Bensason et al.[5] have surveyed the structure and properties of a range of poly(ethylene-*co*-octene)s, as well as other polyolefin copolymers, using transmission electron microscopy, DSC, and mechanical analyses. They classified the copolymers into four different types on the basis of correlations between their morphologies and density/crystallinity, which depends on the comonomer concentration. DSC showed multiple melting endotherms over a broad temperature range. The high end of this transition occurred well below the melting temperature for linear polyethylene, pointing to the existence of only small, imperfect crystallites, such that the crystallinity (ordered phase content) is higher than the estimations based on the heat of fusion and density of the "perfect" polyethylene crystal. In other work, Bensason et al.[6] compared the mechanical properties of several of such LLDPEs and have modeled their stress−strain behavior in terms of a semicrystalline morphology containing two types of network junctions: fringed-micellar crystals and physical entanglements, which serve as slip-links and cross-links, respectively, in the deformation process.

Previous DSC and X-ray analyses[7] of the specific poly(ethylene-*co*-octene) studied in this paper have identified crystallization and melting kinetics for two coexisting ordered structures, on the basis of their different contributions to the reversing and nonreversing components of the modulated heat flow. The WAXS pattern of the isotropic sample showed weak 110 and 200 reflections from the orthorhombic phase plus an additional Bragg reflection at higher *d* spacing superimposed on the amorphous halo, which was assigned to a mesophase. DSC scans showed that the melting process begins immediately above the glass transition at 240 K and is complete at ∼355 K. The observed enthalpy change would correspond to 14% crystallinity at 298 K if the specimen contained large, relatively perfect crystallites of the orthorhombic phase. On cooling from the

* To whom correspondence should be addressed.
† The University of Tennessee.
‡ Case Western University.
§ Permanent address: Karpov Institute of Physical Chemistry, Obukha 10, Moscow 103064, Russia.

10.1021/ma9818331 CCC: $18.00
Published on Web 05/06/1999

isotropic melt, the material crystallized in a nonreversing process, with a relatively sharp exotherm at 318 K, and then continued to crystallize in a partially reversing process until the glass transition was reached. WAXS data recorded at controlled temperature showed that, on cooling the melt, the mesophase appeared after formation of the orthorhombic crystalline phase, i.e., at lower temperatures.

The present paper continues our study of this material using wide- and small-angle X-ray analysis to investigate the apparent three-phase morphology and to see how it changes as a result of deformation.

2. Experimental Section

2.1. Material. The specimens used in this investigation were of a commercially available poly(ethylene-*co*-octene) with 24 wt % (7.3 mol %) 1-octene produced by the DOW Chemical Co. using the INSITE synthesis technology.[8] The molecular and rheological parameters are described elsewhere.[7] The as-received pellets were melt-pressed at 393 K as films of thickness 0.3 mm and cooled slowly (1 K/min) to room temperature. Specimens were stretched uniaxially to 500% and 800% elongation and held at constant length in a frame for X-ray analysis. (Note that under the conditions used the material can be drawn to almost 1200% elongation before break.[9])

2.2. X-ray Diffraction. Wide-angle X-ray diffraction patterns were recorded using pinhole collimation and Ni-filtered Cu Kα radiation, on Kodak direct exposure film, and also using the Siemens Hi-Star general area detector diffraction system. Wide-angle diffractometer scans of scattering by the isotropic sample and by the oriented samples along directions perpendicular and parallel to the draw direction were recorded on a Scintag diffractometer equipped with a solid-state detector, operating in symmetric transmission mode. Small-angle X-ray data were recorded on film using the same pinhole setup and a 30 cm specimen-to-film distance and also using graphite monochromatized Cu Kα radiation with an ORNL area detector at a 5.1 m sample-to-detector distance. All area detector data were corrected for background scattering, detector noise, and absorption.

The degree of crystallinity was estimated from the wide-angle data recorded on the area detector as the ratio of the scattering from the crystalline regions to the total scattering. The specimens showed no evidence for preferred orientation in the plane of the film. For the undrawn specimen, the integration

$$\int I(s,\varphi)s^2\,\mathrm{d}s$$

was over the range of the scattering vector, s, equivalent to Bragg $2\theta = 10-35°$, which contains the three strong $hk0$ reflections. Comparison of the data for the undrawn, drawn, and released specimens showed that the 2θ scattering profiles for their amorphous phases were approximately the same. Thus, the profile for scattering by the amorphous phase in the undrawn specimen was taken as the scattering along the draw direction (meridian) for the 800% drawn sample, since the latter did not contain Bragg reflections within the measured 2θ range. The separation of the scattering into crystalline and amorphous contributions for the undrawn specimen was then achieved by curve fitting.

For the oriented specimens, the amorphous scatter was determined as

$$\int\int I(s,\varphi)s^2 \sin\varphi\,\mathrm{d}s\,\mathrm{d}\varphi$$

where φ is the azimuthal angle, equal to 90° at the equator. The double integration was over s ranging from the equivalent of $2\theta = 10-35°$ and φ from 0 to 180°. The multiplication by $\sin\varphi$ weights the nonequatorial scatter for the effect of orientation, i.e., the sampling of the three-dimensional Fourier transform by the Ewald sphere. There was some φ anisotropy to the amorphous halos, i.e., enhanced intensity in the region of the equatorial Bragg reflection, and this was estimated by extrapolation. (In fact, this anisotropy was relatively small: assumption of an isotropic halo based on a meridional scan reduced the estimated crystallinity by less than 3%.) The total scattering contained in the three equatorial reflections, i.e., that due to the crystalline component, was estimated after subtraction of the extrapolated amorphous background from a sector centered on the equator that extended just beyond the range of φ for the arced reflections.

The longitudinal and lateral crystallite sizes for the orthorhombic crystallites were determined from the integral half-widths of the 002 and 110 reflections using the Scherrer equation, after subtraction of the amorphous background from the area detector data; likewise, the lateral crystallite sizes for the hexagonal phase were determined from its 100 reflection. The measured widths were corrected for instrumental broadening based on data for a standard silicon powder sample, assuming Gaussian profiles.

3. Results and Discussion

Figure 1 shows wide-angle X-ray diffraction data recorded on film for the undeformed original sample (a) and for the same sample after drawing to 500% (b) and 800% elongation (c), and for the latter sample after it was released (d). The released sample contracted to 350% of the original length. The d spacings for the Bragg reflections observed in Figure 1 are given in Table 1, which also includes theoretical d spacings, based on the orthorhombic unit cell with lattice parameters given by Kavesh and Schultz.[11] Figure 2 contains the diffractometer scans of the undrawn (a), 500% drawn (b), and released sample (c), the latter two along the equator and the meridian; the inset shows the data in the range $2\theta = 8.5-24.5°$ at higher magnification. Figure 3 shows the small-angle scattering recorded using the area detector for the unoriented specimen and for the oriented specimens along the draw direction.

In the wide-angle region for the unoriented specimen (Figure 1a) we observe an intense amorphous halo on which are superimposed three Bragg reflections at $d =$ 4.52, 4.15, and 3.77 Å. These features are also visible in the diffractometer data shown in Figure 2a: the first two are well-resolved peaks, and the third is only visible as a shoulder. The second and third reflections are identified as the 110 and 200 reflections of the orthorhombic phase (taking c as fiber axis). At higher angles we also see the weak 020 and 011 reflections predicted for the same structure (see Table 1). The small increase of the d spacings over the theoretical values is consistent with the presence of defects due to the branches.[11,12] When the specimen was drawn to 500% elongation, the three strong Bragg reflections had equatorial disposition (Figure 1b). The d spacings of the orthorhombic structure were almost unchanged, but the first reflection has declined from 4.52 to 4.45 Å. In the data for the 800% drawn sample, the reflections for orthorhombic phase are difficult to resolve, but their d spacings appear to be unchanged. In addition, the reflections are less arced in the 800% than in the 500% drawn sample: the azimuthal half-width of the Bragg peaks had declined from ∼12° to ∼8.5°. On releasing the tension (350% permanent set), the d spacing of the first reflection increased to 4.56 Å, but the others were almost unchanged. The crystallites were still oriented, but the azimuthal half-width increased to ∼31°.

Qualitative inspection of Figures 1 and 2 shows that the relative intensities of the Bragg reflections change during extension, with the first becoming progressively

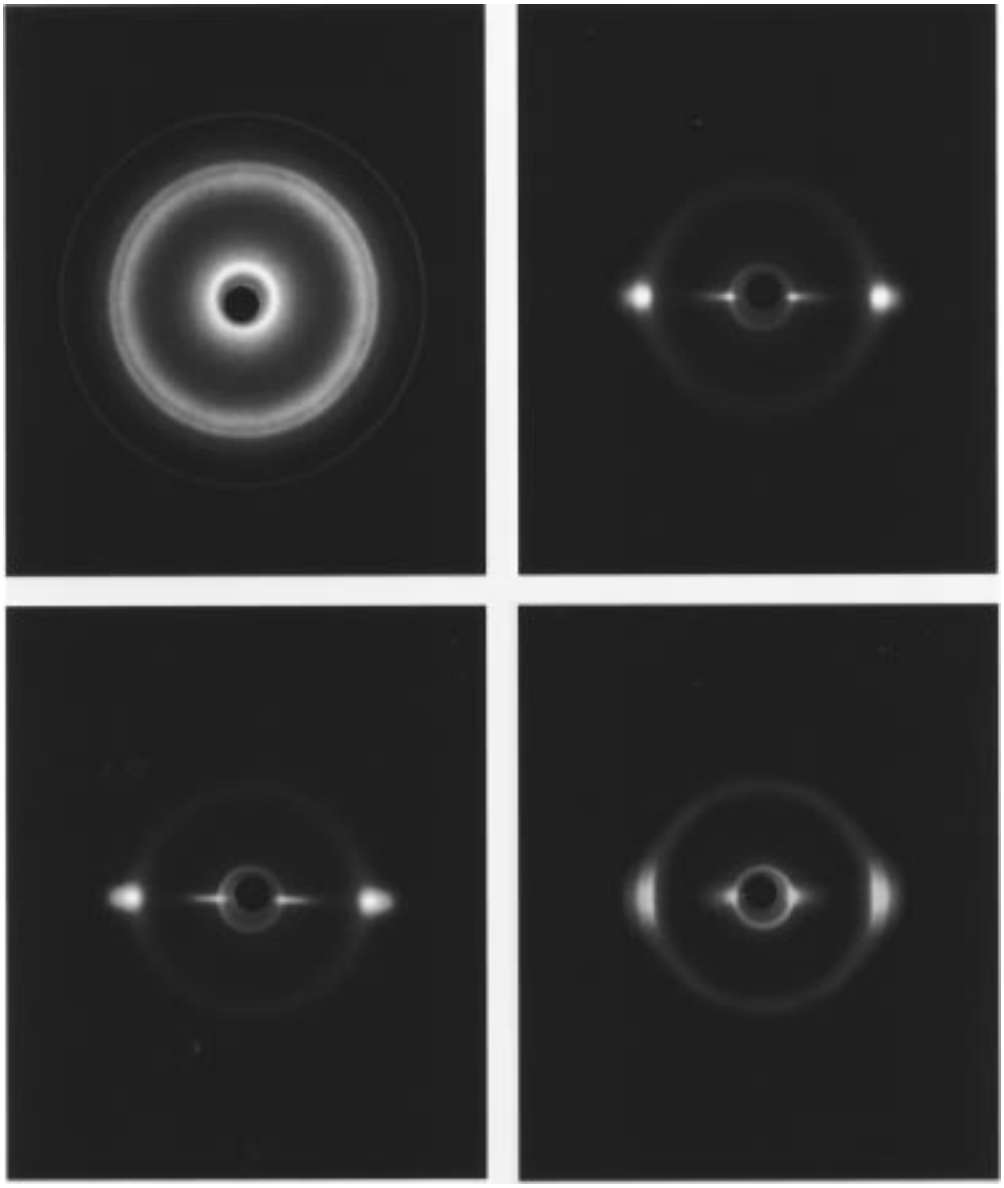

Figure 1. WAXS pattern of poly(ethylene-*co*-octene) recorded on film: (a) undrawn (top left); (b) after drawing to 500% elongation (top right); (c) after further drawing to 800% elongation (bottom left); (d) upon releasing after 1 week at 800% elongation (bottom right). (Note that the inner rings and streaks are due to white radiation.)

Table 1. Wide-Angle *d*-Spacings of Poly(ethylene-*co*-octene)

	d-spacing/Å			
(*hkl*)	undrawn	500% drawn	released	theoretical[11]
	4.52 ± 0.02	4.45	4.56	
(110)	4.15 ± 0.01	4.14 ± 0.01	4.18	4.09
(200)	3.77 ± 0.01	3.76 ± 0.01	3.77	3.69
(020)	2.48	2.48 ± 0.01	2.50	2.46
(011)	2.26	2.246 ± 0.005		2.25
(002)		1.274 ± 0.005	1.266	1.265

more intense. It is also apparent that the first reflection broadens in the 2θ direction, suggesting a decrease in the crystallite size, whereas the width of the second reflection is largely unaffected. These observations are consistent with the presence of two crystalline structures within the sample, for which the relative proportions and crystallite sizes change during deformation. The first reflection is not predicted for the orthorhombic form and could originate from two other polyethylene structures: the monoclinic (or triclinic) form[13] or the hexagonal form. The strong 010 reflection of the monoclinic form is reported to be at $d = 4.55$ Å by several authors;[14−16] it also gives 200 and reflections that would be overlapped with the 200 reflection for the orthorhombic phase in the isotropic sample. However, the monoclinic form has never been observed under the present conditions, and there is no reason to suggest that its existence might be favored by the presence of the side groups in this particular poly(ethylene-*co*-octene). The more likely explanation is that the first reflection is due to the presence of hexagonal crystallites. The 100 reflection for the hexagonal form has been observed at elevated temperatures in oriented polyethylene[14,17] but, more importantly, has been unambiguously identified as the source of the reflection at $d =$ 4.43 Å in the data for isotropic 75/25 copoly(ethylene/propylene) at room temperature.[18] Thus, it appears likely that the first observed reflection is due to the presence of some hexagonal structure that coexists along with the orthorhombic and amorphous phases. We see a second-order (200) reflection at $d \sim 2.25$ Å, but the 110 reflection predicted at $d \sim 2.61$ Å is not detected.

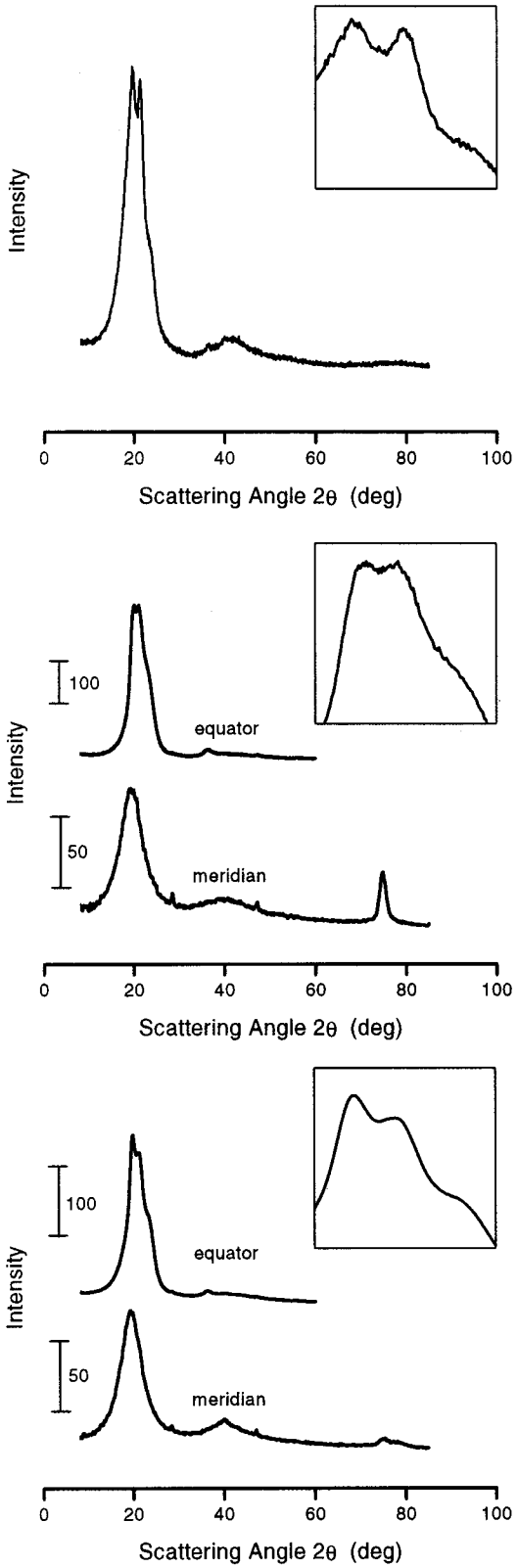

Figure 2. Diffractometer scans of poly(ethylene-*co*-octene) (intensity versus scattering angle 2θ): (a, top) undrawn; (b, middle) after drawing to 500% elongation, recorded perpendicular and parallel to the draw direction; (c, bottom) upon releasing after 1 week at 800% elongation, recorded perpendicular and parallel to the original draw direction.

However, the latter reflection is weak in the much more detailed WAXS data for the hexagonal phase for linear polyethylene preparations at elevated temperatures and thus would probably not be resolved here. The hexagonal structure for linear polyethylene is a mesophase at room temperature: it probably occurs in these poly(ethylene-*co*-octene) specimens in order to accommodate the side chain defects. The decline in the *d* spacing from 4.52 to 4.45 Å that occurs on elongation suggests that alignment of the chains allows for closer packing. In the discussion that follows we will refer to this second ordered phase as the hexagonal form, even though unequivocal identification has not been achieved.

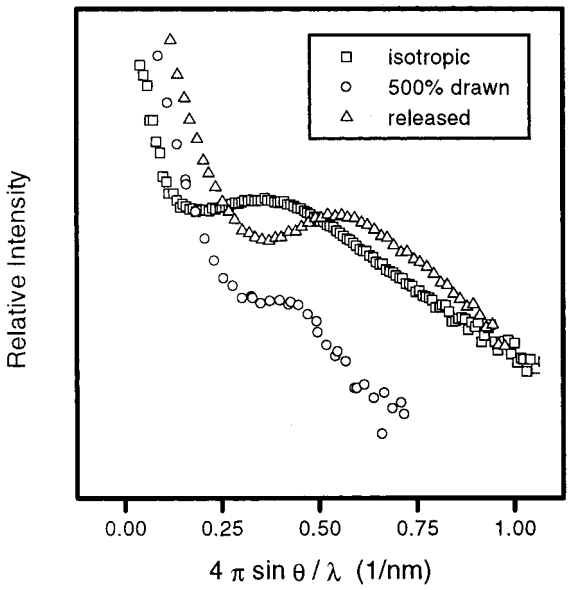

Figure 3. SAXS diagrams of poly(ethylene-*co*-octene): (a, □) undrawn; (b, ○) after drawing to 500% elongation, recorded along the draw direction; (c, △) upon releasing after 1 week at 800% elongation, recorded along the draw direction.

Review of the data in Figure 1 also shows that the intensities of the Bragg reflections relative to that of the amorphous halo appear to increase with extension, suggesting that crystallinity increases as the chains become more oriented. Separation of the wide-angle data for the isotropic sample by curve fitting yields a degree of crystallinity of 28 ± 5%. Needless to say, many caveats need to be attached to this calculation, given the assumptions with regard to the amorphous background and the degrees of freedom in fitting the peak positions and peak widths for the Bragg reflections. So its main utility is as a benchmark for comparison with the data for the deformed specimens. Nevertheless, whatever limits are placed on this analysis, it is clear that the degree of crystallinity is higher than that derived from the DSC melting enthalpy (14%, when using 290 J/g as heat of fusion of the crystalline phase); i.e., the specimen contains a higher proportion of crystals, but these are relatively small and distorted. The small-angle data for the undeformed specimen (Figure 3, curve a) contains a single maximum at a long period $L \approx 175$ Å, suggesting that at least some of the specimen consists of periodic stacks of crystalline and amorphous regions.

In the wide-angle data of the 500% elongated sample (Figure 1b), the crystalline contribution is almost entirely in the equatorial region (perpendicular to the draw direction). The lateral crystallite sizes determined from the 2θ half-widths are ~100 Å for both the hexagonal and orthorhombic forms and are essentially unchanged from those in the undeformed sample. However, the first reflection appears to be more intense than the second, whereas they previously had ap-

proximately the same intensity, and the qualitative impression is that the degree of crystallinity has increased due to creation of more of the hexagonal form. The crystalline scatter is contained almost entirely in the first three equatorial reflections: the layer line reflections for the orthorhombic form contribute no more than 1−2% of the total and can be neglected. Thus, we determined the degree of crystallinity on the basis of the integrated intensity of the three equatorial reflections compared to that of the amorphous halo, with angular corrections as described in the Experimental Section. The crystallinity obtained for the 500% elongated sample was 57 ± 5%.

The wide-angle data in Figure 1b also contain the 020, 011, 111, and 201 reflections for the orthorhombic form. No layer line reflections due to a second phase are detected, which is consistent with the presence of the hexagonal structure, for which at best only layer line streaks are observed. The 2θ angular width of the 002 reflection at $d = 1.27$ Å yields an axial crystallite size of ∼65 Å. This length exceeds the average segment length between side chains, which would be ∼35 Å if the sequence distribution is random. It is, however, much less than the lateral crystallite size (∼100 Å) which, together with our observation of an arced small angle meridional maximum at $L \approx 140$ Å, is consistent with the existence of some stacked lamellar crystallites.

When the copolymer is stretched to 800% elongation, the orientation of the crystallites is increased, and there are also striking increases in the width and relative intensity of the first equatorial reflection (Figure 2c). Line broadening measurements show that the lateral crystallite size for the hexagonal form has fallen to ∼50 Å. The relative intensity of 110 reflection for the orthorhombic form is weaker than in Figure 1a,b; 011 and 200 reflections are detected, but they are also weaker and broader than those seen at 500% elongation. The crystallinity is estimated to be 58 ± 5%, essentially unchanged from that measured at 500% elongation. It can be concluded that the deformation has proceeded via the destruction of some of the orthorhombic crystallites and the creation of new, hexagonal structures which, however, have much smaller lateral widths. The small-angle data for this specimen consist of a weak, meridional arc at $L \approx 130$ Å, consistent with a lower proportion of stacked lamellae.

Estimates of the degree of crystallinity ranging from ∼25% to ∼50% require a structure in which the majority of the ordered regions must include chain segments with side chains. It seems reasonable that the orthorhombic crystallites might consist of segments with fewer side chains defects, which would be consistent with the fact that they comprise a relatively minor fraction of the whole when the crystallinity is ∼50%. Nevertheless, the side chains could probably be incorporated relatively easily into the hexagonal structure. Even for linear polyethylene chains (at high temperature) the chain conformation, although extended, is believed to be irregular, and there is no three-dimensional register. The studies by Ungar and Keller[19] have shown that the hexagonal mesophase for linear polyethylene is metastable at room temperature. However, it is stable for copoly(ethylene/propylene);[18] i.e., the presence of the side chain defects will stabilize the hexagonal form at lower temperatures. The defects will also limit lateral growth, resulting in the lower size for the new crystallites formed at high deformation.

On releasing the tension, the fully stretched specimen contracts to 350% extension; i.e., there is a permanent set characteristic of a thermoplastic elastomer. From the wide-angle data, the estimate of the degree of crystallinity is 36 ± 5%; i.e., the crystallinity has fallen back toward the value for the undeformed specimen. The relative intensity of the first equatorial reflection has declined, indicating that this reduction in crystallinity is due mainly to loss of the small hexagonal crystallites formed during elongation. Note that the *d* spacing for the 100 reflection for the hexagonal form has increased, and the lateral crystallite widths for both forms have been restored to ∼100 Å. Nevertheless, the relative intensity of the first equatorial is still higher than that of the second, indicating that the proportion of hexagonal crystallites exceeds that in the isotropic and 500% stretched specimens. The small-angle X-ray data for this specimen are a distinct four-point diagram with $L \approx 115$ Å; the angle of inclination of the crystalline interface is ∼25°, pointing to a chevron morphology in which the surfaces of the lamellae are inclined to the chain axis/draw direction. The sharpness of the pattern points to a relatively well-defined surface for the lamellae, as would occur in chain folded orthorhombic crystallites, and these structures could also be present in the undeformed specimen.

4. Conclusions

Analysis of the structure of poly(ethylene-*co*-octene) containing 7.3 mol % 1-octene by wide- and small-angle X-ray techniques reveals a distinct three-phase structure in isotropic and oriented samples. In addition to the amorphous phase, there are two ordered phases: one of these is the orthorhombic structure, and the other is most likely the hexagonal mesophase. The latter is stable at room temperature and probably accommodates the side chains which are more likely to be excluded from the orthorhombic crystalline phase. Stretching the isotropic sample leads to orientation and an increase of the proportion of hexagonal form, while the orthorhombic and amorphous fractions are both reduced. The new hexagonal regions are smaller than those detected in the original unoriented specimen and are probably highly distorted due to incorporation of the side chains. The data point to a degree of crystallinity of ∼28% for the original specimen, and this increases to ∼50% at 500% and 800% extension. These figures are all considerably higher than the DSC crystallinity (∼14% for the undeformed sample), consistent with the existence of relatively distorted crystallites. Thus, it appears that extension to 800% has resulted in removal of chains from the orthorhombic crystallites, and these and/or other chains originally in the amorphous regions then undergo stress-induced crystallization. Most but not all of these hexagonal crystallites revert to amorphous or orthorhombic structures on releasing the stress.

Acknowledgment. This work was supported by the Division of Materials Research, NSF, Polymers Program, Grant DMR-9703692, and the Division of Materials Sciences, Office of Basic Energy Sciences, U.S. Department of Energy at Oak Ridge National Laboratory, managed by Lockheed Martin Energy Research Corp. for the U.S. Department of Energy, under Contract DE-AC05-96OR22464.

References and Notes

(1) McFaddin, D. C.; Russell, K. E.; Wu, G.; Heyding, R. D. *J. Polym. Sci., Polym. Phys.* **1993**, *31*, 175.

(2) Mathot, V. B. F.; Pijpers, M. F. J. *J. Appl. Polym. Sci.* **1990**, *39*, 979.
(3) Mathot, V. B. F.; Scherrenberg, R. L.; Pijpers, M. F. J.; Bras, W. *J. Therm. Anal.* **1996**, *46*, 681.
(4) Minick, J.; Moet, A.; Hiltner, A.; Baer, E.; Chum, S. P. *J. Appl. Polym. Sci.* **1995**, *58*, 1371.
(5) Bensason, S.; Minick, J.; Moet, A.; Chum, S.; Hiltner, A.; Baer, E. *J. Polym. Sci., Polym. Phys.* **1996**, *34*, 1301.
(6) Bensason, S.; Stepanov, E. V.; Chum, S.; Hiltner, A.; Baer, E. *Macromoelcules* **1997**, *30*, 2436.
(7) Androsch, R. *Polymer* **1999**, *40*, 2805.
(8) Dow Plastics, Product Information, Engage Polyolefine Elastomers.
(9) Androsch, R., unpublished data.
(10) Alexander, L. E. *X-ray Diffraction Methods in Polymer Science*; Wiley-Interscience: New York, 1969.
(11) Kavesh, S.; Schultz, J. M. *J. Polym. Sci., Polym. Phys.* **1970**, *8*, 243.
(12) Balta-Calleja, F. J.; Vonk, C. G. *X-ray Scattering of synthetic Polymers*; Elsevier: Amsterdam, 1989.
(13) Wunderlich, B. *Macromolecular Physics;* Academic Press: New York, 1973; Vol. 1.
(14) Pennings, A. J.; Zwijngenburg, A. *J. Polym. Sci., Polym. Phys.* **1979**, *17*, 1011.
(15) Seto, T.; Hara, T.; Tanaka, K. *Jpn. J. Appl. Phys.* **1968**, *7*, 31.
(16) van Aerle, N. A. J. M.; Braam, A. W. M. *J. Mater. Sci.* **1988**, *23*, 4429.
(17) Chvalun, S. N.; Bessonova, N. L.; Konstantinopolskaja, M. B.; Bakeev, N. F. *Dokl. Akad. Nauk SSSR* **1987**, *194*, 1418.
(18) de Ballasteros, O. R.; Auriemma, F.; Guerra, G.; Corradini, P. *Macromolecules* **1996**, *29*, 141.
(19) Ungar, G.; Keller, A. *Polymer* **1980**, *21*, 1273. Ungar, G. *Polymer* **1980**, *21*, 1278; Ungar, G.; Grubb, D. T.; Keller, A. *Polymer* **1980**, *21*, 1284.

MA9818331